LOW-VOLTAGE SCRATCH-DRIVE MICRO-SCALPELS CONTROLLED BY A BINARY-ENCODED SIGNAL

Jung H. Cho and Mark G. Arnold
Lehigh University, Bethlehem, Pennsylvania, U.S.A.

Keywords: MEMS, SDA, Micro-robot, Micro-scalpel.

Abstract: A novel approach to applying multi-stylus MEMS SDA Scratch-Drive-Actuator (SDA) micro-robots to aid in the diagnosis and treatment of dermatological conditions is presented. The operation of MEMS SDA has been well demonstrated by the research of (Donald et al., 2008) (Donald et al., 2006)(Donald et al., 2003). We assume that such SDAs may be applied to the skin and powered by a bandage-like substrate. A method of controlling the turning operation of MEMS SDA Scratch-Drive-Actuator (SDA) micro-robots has been developed previously by our research: adding an additional stylus arm to control left and right rotation as well as using both arms to halt. In order to control multiple micro-robots without the complication of different stress curling that requires high voltages incompatible with dermatological applications, an alternative solution of controlling electrical connection between the parallel-plate body and the stylus arms is presented that uses a binary-encoded signal. Also an additional beam added to the body of SDA to be used as micro-scalpel can be controlled by this same signal

1 INTRODUCTION

Micro-Electro-Mechanical Systems (MEMS) are now commonly used in mirrors, optical gratings, variable capacitors, and accelerometers. Micro-robots fabricated from MEMS need four basic components: power supply, sensors, control and motion transducers. One of the most widely researched MEMS transducer is the Scratch Drive Actuator (SDA), which is an L-shaped beam of poly-silicon that moves across a powered substrate as a voltage is applied and released. The electrostatic attraction between the substrate and the poly-silicon deforms the “L” shape, making the SDA act like a spring, which is released when the external voltage is removed. An un-tethered micro-robot has been developed (Donald et al., 2003) utilizing such electrostatic actuation. Although this design has only been demonstrated in isolation from any biological material on top of the artificial environment of a powered substrate, this position paper argues that for some dermatological procedures, SDA-based micro-robots, which are placed between a flexible (bandage-like) powered substrate and the skin, may be a useful diagnostic aid and may also enhance surgical precision.

The MEMS micro-robot built by (Donald et al., 2006) has a dimension of 60μm by 250μm by 10μm. Figure 1 shows the structure of this device proposed in (Donald et al., 2006), which propels itself forward (moving the brushing towards the viewer in Figure 1) along the powered surface by bending and releasing its large rectangular scratch-drive plate (Donald et al., 2006). A stylus steering arm provides single-direction turning capability (counterclockwise as shown in Figure 1) by holding the robot stationary at the dimple while the release of the main plate provides torque. The approach taken by (Donald et al., 2008) encodes the four micro-robot states (stylus up plate up, stylus up plate down, stylus down plate up, stylus down plate down) with four different voltage levels. Donald et al. have generalized the multi-voltage-level encoding (Donald et al., 2008)(Donald et al., 2006) to control multiple robots from a single external signal by using hysteresis built into the design of each SDA (different chip dimensions corresponding to different activation voltages). Having multiple robots operating simultaneously would give more information and greater control to the surgeon, but with the (Donald et al., 2008) multi-voltage encoding, the full voltage swing may be hundreds of volts, a level which may not be safe or comfortable for the patient.

Cho J. and Arnold M. (2010).
LOW-VOLTAGE SCRATCH-DRIVE MICRO-SCALPELS CONTROLLED BY A BINARY-ENCODED SIGNAL.
In *Proceedings of the Third International Conference on Biomedical Electronics and Devices*, pages 219-223
DOI: 10.5220/0002760202190223

The approach we propose is different. Unlike the multiple-robot system of (Donald et al., 2008) in which each robot obtains its motion command via a unique external voltage, we assume that the robots have on-board digital logic capable of receiving a binary-encoded command over a series of clock cycles, and that each possible motion for each robot has a unique binary code. In our proposal, each robot will have identical SDA dimensions, and use digital logic to make the behavior of each robot unique. With the proper choice of geometry, scratch-drive activation can happen around ten volts. The additional voltage swing needed to transmit our binary code is on the order of a volt, so that the total voltage of the signal applied to the patient skin will be imperceptible. Since there can be a measurable difference in conductance between normal and tumorous tissue (Smith et al., 1986), having a large swarm of robots performing such measurements in real time will help the surgeon minimize the amount of tissue removed.

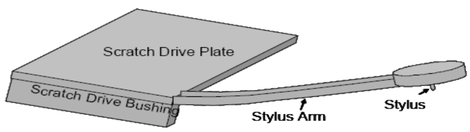

Figure 1: Illustration of MEMS Micro-robot (Donald et al. 2006).

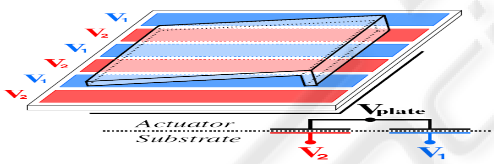

Figure 2: Illustration of SDA on power grid (Donald et al., 2006).

2 DUAL-STYLUS SDA WITH MICRO-SCALPEL

Figure 2 shows the schematic of the capacitively-coupled power grid used by (Donald et al., 2006). By using these electrodes, the SDA operates by attracting its body to the electrodes when external high voltage is applied, and jumping like a spring when the voltage is removed. Therefore, in order to be propelled, a clock-like voltage waveform has to be applied (Donald et al., 2006). In our novel approach, the voltage on the scratch-drive plate can also be used to supply power to on-board digital logic as shown in Figure 3. We have demonstrated this in our previous research by developing a Verilog-A model of the SDA and applying voltage regulation to provide adequate voltage swing for 1V 40nm CMOS standard-cells from the plate voltage as a power (Cho and Arnold, 2009).

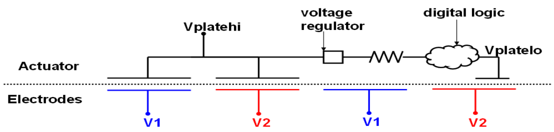

Figure 3: Equivalent circuit showing $V_{platehi}$ and $V_{platelo}$.

In order to change direction, Donald's SDA (Donald et al., 2006) uses a stylus steering arm and requires higher voltage to achieve pull-in or snap-down voltage (Donald et al., 2006) necessary to make contact with the substrate. This requirement introduces multi-voltage level encoded power waveform, which is used by Donald's SDA. In order for many SDAs to interact as shown in Donald's (Donald et al., 2008), all of them need to have different stresses applied during fabrication so that the stylus arms can curl differently in order to vary the pull-in voltage (Saha et al., 2006). Our novel approach is to apply a switch or a large transistor to control the conductivity between the stylus arm and the parallel-plate body. This eliminates the step needed for different stress curling, and one voltage waveform can be used to supply power to different SDA micro-robots. We

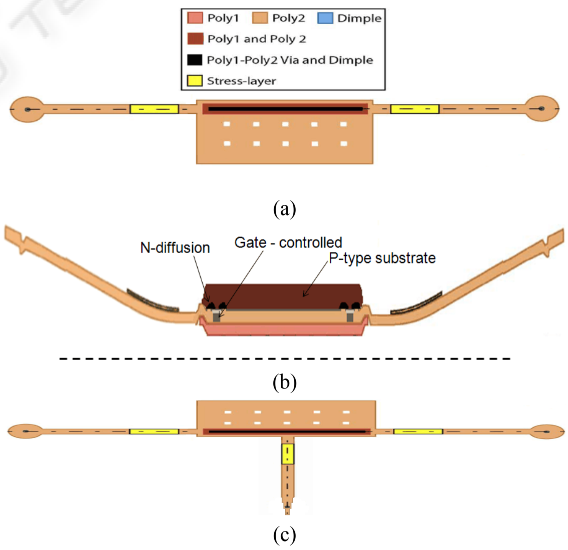

Figure 4: (a) Top view of proposed SDA modification from (Donald et al., 2006) in order to perform both left and right turn. (b) Frontal view of proposed SDA modification from (Donald et al., 2006) in order to control pull-in/snap-down voltage of the stylus steering arms. (c) Top view of proposed SDA modification from (Donald et al., 2006) in order to include micro-scalpel.

also added a second arm, as seen in Figure 4a and 4b, to be able to turn left and right, and use both arms to enforce a stationary position. Figure 4c illustrates the addition of a micro-scalpel beam which can be used to probe or cut samples as necessary.

The modified SDA consists of 3 components which are left and right stylus beams and parallel-plate capacitor body. Figure 5 shows the high-level illustration of this structure. The capacitance across the parallel-plate is the most dominant energy storage part of this circuit. Since the V1 and V2 electrodes are uniformly covering the whole area of the parallel-plate, the voltage across the plate can be summarized as (Donald et al., 2003),

$$V_{plate} = \frac{V_1 C_1 + V_2 C_2}{C_1 + C_2} \qquad (1)$$

When both arms are connected to the parallel plate body, the voltage across the beams ($V_{left\text{-}arm}$ and $V_{right\text{-}arm}$ in Figure 6), would be the same compared to V_{plate}.

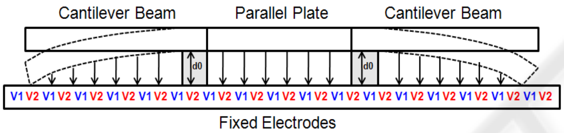

Figure 5: Deformation in cantilever and parallel plate due to applied voltage.

When the beams are electrically disconnected, then each stylus beam becomes a well-known MEMS cantilever beam (Saha et al., 2006)(Wei et al., 2002). We applied the modeling technique and equations from Wei's research (Wei et al., 2002) to build a Verilog-A model to work with our previously developed model of SDA. Figure 6 shows a different voltage across the beams and the plate when arms are disconnected. Under ideal fabrication process, $V_{left\text{-}arm}$ and $V_{right\text{-}arm}$ would be identical.

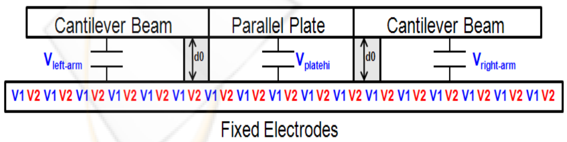

Figure 6: Illustration of different voltage across the beams and the plate capacitor due to disconnection from the parallel plate body.

$V_{left\text{-}arm}$, $V_{right\text{-}arm}$ and V_{plate} represent the pull-in voltage needed to cause attraction. This equation is defined as (Saha et al., 2006),

$$V_{PI} = \sqrt{\frac{8kd_0{}^3}{27\varepsilon_0 A}} \qquad (2)$$

Here 'k' is the spring constant, 'd_0' is the initial gap height and 'A' is the area coverage of the cantilever. Previous research (Donald et al., 2008) influenced V_{PI} based on careful selection of these parameters, 'k' and 'd_0'. We will show that these parameters can remain constant, and by simply connecting and disconnecting the cantilever arms from the parallel plate body electrically we can control the V_{PI}. And we will use this control in section V to present a parallax algorithm which can be used to guide the micro-robots with an on-board algorithm that does not need external control.

3 INTERMITTENT POWER AND MAGNETIC TUNNEL JUNCTION NON-VOLATILE FLIP-FLOP

As described in the previous section, a MEMS SDA micro-robot is driven by external voltage using the electrodes underneath to create an electrostatic field and to cause actuation which is transferred into forward or turning motions. This external voltage is applied in clocked fashion around 1 KHz, which we will refer to as a major cycle. Since the voltage is applied intermittently, there needs to be a solution to hold important states needed for continuous operation of the on-board logic. This leads to applying non-volatile flip-flops developed using Magnetic- Tunnel-Junction (MTJ) technology (Zhao and Belhaire, 2007). This flip-flop works like a standard flip-flop but information is stored in MTJs; therefore, when the SDA's major power cycle occurs, the MTJ flip-flop restores to its previously saved state. In order to demonstrate this we simulated the MTJ flip-flop (Zhao and Belhaire, 2007) and developed Verilog-A model of a dynamic storage behavior of MTJ. We then simulate this MTJ flip-flop in Cadence AMS environment to co-simulate both transistors and Verilog-A/Verilog-AMS models.

4 DUAL-STYLUS SDA SIMULATION

In order to demonstrate the operation of the dual-stylus SDA, we have developed a Verilog-A model to capture the voltage across the beams and the parallel plate. First, we verified that V_{plate} can still be used to supply power to the on-board CMOS digital logic when two arms are connected and disconnected. We have chosen 4 bit counter to demonstrate the operation along with storage behavior of the MTJ flip-flop from section III. A 4-bit counter was synthesized from Verilog RTL into 40nm standard cells using positive edge flip-flops and they were replaced with a MTJ non-volatile flip-flop Verilog-A/AMS model. We then integrated all the models to simulate in the Cadence AMS environment. The setup is shown in Figure 7. This type of system-level simulation utilizing Verilog-A/Verilog-AMS models has been accepted in research (Mateu and Moll, 2007).

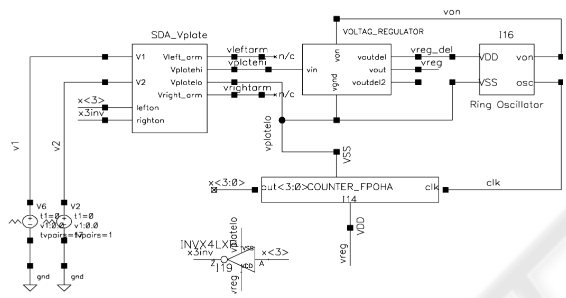

Figure 7: Top level simulation setup.

Figure 8 shows the simulation result of the counter. The first waveform shows the intermittently-applied and voltage-regulated output to drive the ring oscillator and the counter. The next 4 waveforms are output of the counter `x[3:0]`. As the power was removed, the counter state was saved in the MTJ flip-flop as 0011. When the power returned, it restored the state 0011 and continued counting. This result provided assurance that more elaborate state machines can be pursued with this architecture.

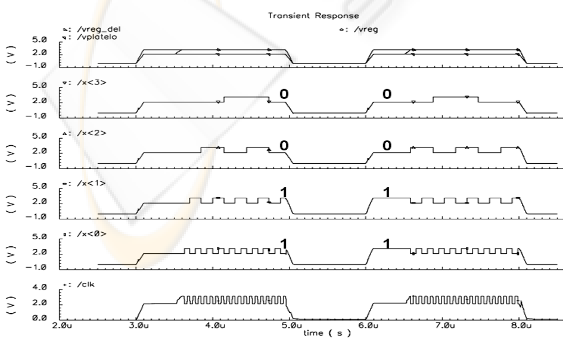

Figure 8: Simulation result of 4-bit counter.

Then, we used the counter output bit x[3] to control the left stylus and inversion of x[3] to control the right stylus. Figure 9 shows the voltage across $V_{left-arm}$ and $V_{right-arm}$ changing as x[3] toggles. As expected, V_{plate} remained constant during x[3] change since it has the most capacitance to hold the charge.

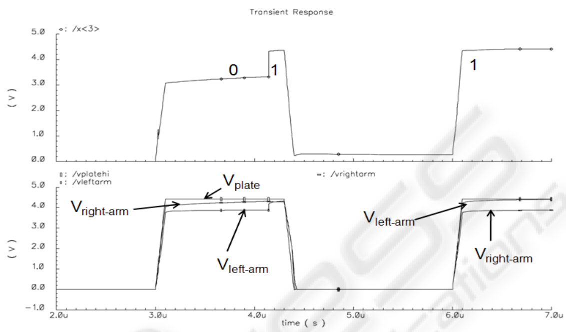

Figure 9: $V_{left-arm}$, $V_{right-arm}$ and V_{plate} result.

5 BINARY-ENCODED CONTROL

Section II through IV described support circuits developed in order to control one dual-stylus micro-robot. However, in order to control multiple micro-robots there needs to be a global communication channel necessary to operate them. We propose that using the V1/V2 power grid described in section II as a communication channel would be a solution to this problem. The original V1 or V2 functional goal has not changed and will continuously provide propulsion and supply power to CMOS digital logic on board the micro-robot. The architecture we propose is while V1 or V2 is in a high state and supplying power to on-board logic we can apply higher frequency serial data onto V1 or V2 to convey control information to each of the micro-robots on the power grid. This idea is in line with technology used to transfer data through power-lines using frequency division multiplexing (Hensen, 1998). Figure 10 illustrates an example of using an eight-bit binary signal to control the motion of four robots (from a swarm that could contain up to thirty-two robots). In this example, none of the micro-scalpels are engaged (indicated by the most significant bit of the 8-bit code); each robot number (indicated by the middle 5-bit value) performs a different move (indicated by the least two significant bits).

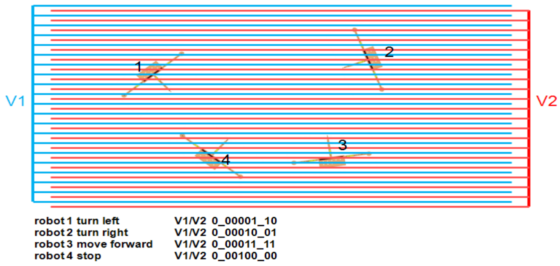

Figure 10: V1 / V2 are used as channels to apply binary encoded controls to each micro-robot.

Each micro-robot is assigned a unique 5-bit number and as part of the on-board logic there is an 8-bit UART which recovers the serial communication and programs each micro-robot for the operation it needs to perform. When a particular micro-robot receives a 5-bit number that does not match its assigned robot number, the robot in question ignores the three command bits. If, on the other hand, the 5-bit numbers match, the robot in question will latch the three command bits into MTJ flip-flops so that at the next major cycle the robot in question will perform the command specified. The UART is clocked every minor cycle, which operates at a much higher frequency than the major cycle. Since transmitting each 8-bit code requires a start and stop bit, the bandwidth required on the global communications channel for a swarm of 32 robots is at least 10*32=320 times the major cycle, and the UART operates at some multiple of this. For example, if the major cycle is 1 KHz and the UART requires 8 minor cycles per bit received, the minor cycle needs to be about 2.5 MHz because the channel needs to transmit at least 320,000 bits/second.

6 CONCLUSIONS

We have proposed a novel approach of applying MEMS SDA micro-robots to assist in dermatological procedures on the assumption power may be applied via a bandage-like substrate. We discussed features needed on a MEMS micro-robot to achieve this. It needs improvement from Donald et al. (Donald et al., 2006) to provide uniform control for turning MEMS SDAs using a much lower voltage signal that used by Donald et al. By adding an additional stylus arm the robot can now turn both left and right as well as use both arms to stop. A third stylus arm provides a micro-scalpel. Fabricating a transistor connection between each stylus and the parallel-plate body allows the micro-robot to control the pull-in voltage. Using this control capability, we also presented a new approach to using the power grid to communicate to each micro-robot using a binary-encoded signal which operates at much lower voltages than previous multi-robot SDA systems.

REFERENCES

Bruce R. Donald, Christopher G. Levey, and Igor Paprotny, 2008.

Planar Microassembly by Parallel Actuation of MEMS Microrobots. In *IEEE – Journal of Microelectro-mechanical Systems*, vol. 17, no. 4.

Bruce R. Donald, Christopher G. Levey, Craig D. McGray, Igor

Paprotny, and Daniela Rus, 2006. An Untethered, Electrostatic, Globally Controllable MEMS Micro-Robot. In *IEEE – Journal of Microelectro-mechanical Systems*, vol. 15, no. 1.

Bruce R. Donald, Christopher G. Levey, Craig D. McGray, and

Daniela Rus, 2003. Power Delivery and Locomotion of Untethered Micro-actuators. In *IEEE – Journal of Microelectromechanical Systems*, vol. 12, no. 6.

W. Zhao, E. Belhaire, C. Chappert, 2007. Spin-MTJ based

Non-Volatile Flip-Flop. In *International Conference on Nanotechnology*.

Loreto Mateu and Francesc Moll, 2007. System-level Simulation

of a Self-powered Sensor with Piezoelectric Energy Harvesting. In *International Conference on Sensor Technologies and Applications*.

Shimul Chandra Saha, Ulrik Hanke, Geir Uri Jensen, and

Trond Saether, 2006. Modeling of Spring Constant and Pull-down Voltage of Non uniform RF MEMS Cantilever. In *Behavioral Modeling and Simulation Workshop, Proceedings of the 2006 IEEE International*, pp. 56-60.

Leow Cheah Wei, Abu Baker Mohammad and

Norazan Mohd. Kassim, 2002. Analytical Modeling For Determination Of Pull-In Voltage For An Electrostatic Actuated MEMS Cantilever Beam. In *Proceedings of ICSE2002*.

Smith, Susan Rae, Foster, Kenneth R., Wolf, Gerald L., 1986.

Dielectric Properties of VX-2 Carcinoma Versus Normal Liver Tissue. In *IEEE Transactions on Biomedical Engineering*, BME-33, 5, 522-524.

C. Hensen, 1998. Data transmission applications via low voltage

power lines using OFDM technique. In *1998 IEEE 5th International Symposium on Spread Spectrum Techniques and Applications*, 1, 210 – 214.

Jung H. Cho and Mark G. Arnold, 2009. Powering Embedded

CMOS Logic on MEMS-based Micro-Robots. In *IEEE International Behavioral Modeling and Simulation Conference*, 73-77.